Journal of Optics (September 2025) 54(4):1724–1731
https://doi.org/10.1007/s12596-024-02093-5

RESEARCH ARTICLE

A novel fiber Bragg grating acceleration sensor based on the double-hinge structure

Yudan Sun[1] · Binwen Li[2] · Wenjing Li[2] · Qiang Liu[2] · Tianshu Fu[2] · Wei Liu[2] · Paul K. Chu[3] · Chao Liu[2]

Received: 9 December 2023 / Accepted: 18 July 2024 / Published online: 30 July 2024

Abstract
A novel fiber Bragg grating (FBG) acceleration sensor with the double-hinge structure is designed and analyzed. The influence of the structural parameters on the sensor characteristics is determined theoretically and the structural parameters are optimized by the finite element method. By adopting the optimal structural parameters, the double hinge structure is prepared with 304 stainless steel and the FBG which is pasted on the surface of the two hinges is used to measure the acceleration sensing characteristics. Experimental results reveal flat response in the vibration frequency range of 50 ~ 600 Hz and sensitivity of 300 mV/g at 600 Hz. At the same time, the operational frequency range and sensitivity can be adjusted to accomplish a wide dynamic range and high sensitivity by optimizing the hinge parameters.

Keywords Acceleration sensor · FBG · Double hinge · Vibration measurement

Introduction

It is crucial to monitor vibrations in seismic studies, geological exploration, health evaluation, and mechanical systems. Because the traditional electrical vibration sensors are not stable in harsh environments, efforts have been made to develop optical fiber vibration sensors which have advantages such as the small size, light weight, acid and alkali corrosion resistance, anti-electromagnetic interference, and high sensitivity. In order to monitor vibrations accurately, optical fiber acceleration sensors such as Mach-Zehnder acceleration sensors [1], Fabry-Perot acceleration sensors [2], Michelson acceleration sensors [3], and fiber Bragg grating acceleration sensors [4] have been proposed. However, although the interferometric acceleration sensors have high sensitivity, the measurement range is small and it is susceptible to noise interference. In contrast, FBG acceleration sensors have drawn a great deal of attention due to the stable performance, high sensitivity, wide measurement range, distributed measurement [5], and wavelength multiplexing [6].

In general, an acceleration sensor consists of an inertial mass block, elastic element, damped system, and sensitive element. In optical fiber sensors, FBGs are used as the sensitive elements to measure displacements of the inertial mass caused by the external vibration mass. The performance of acceleration sensors depends on the structure and the common elastic elements include the beam type [7], diaphragm type [8], hinge type [9], and cylinder type [10]. The cylinder structure has good anti-interference ability and the FBG is packaged in a uniform force, but it is difficult to improve the sensitivity. The diaphragm structure has adjustable sensitivity but the packaging process is complex. Although the beam structure is simple, the detection frequency band is narrow and the anti-interference ability is weak. Compared to these structures, the hinge structure delivers a better comprehensive performance including high sensitivity, large flat response range and FBG acceleration sensors based on the hinge structure have been studied recently [11]. Zhang et al. [12] have reported a two-dimensional FBGs acceleration

✉ Qiang Liu
nepulq@126.com

✉ Chao Liu
msm-liu@126.com

1 College of Mechanical and Electrical Engineering, Daqing Normal University, Daqing 163712, China

2 School of Physics and Electronic Engineering, Northeast Petroleum University, Daqing 163318, China

3 Department of Physics, Department of Materials Science and Engineering, Department of Biomedical Engineering, City University of Hong Kong, Tat Chee Avenue, Kowloon, Hong Kong, China

sensor consisting of a universal flexible hinge and two FBGs that show resonant frequencies of 1050/1060 Hz and sensitivity of 13.1/12.0 pm/g in the X and Y directions, respectively. Qiu et al. [13] have studied the FBG acceleration sensor comprising three mass blocks and four flexible hinges and the experimental results disclose that the measurement range of the accelerometer is 50 ~ 800 Hz and the sensitivity is approximately 29 pm/g. Wei et al. [14] have improved the hinge structure and designed a two-dimensional FBG acceleration sensor based on the multi-axis flexible hinge. The stable operating frequency range of the sensor is 5–170 Hz and the acceleration sensitivity is 220 pm/g, but the operating frequency range is small. Yan et al. [15] have reported an FBG accelerometer composed of two straight circular flexible hinges connected in parallel with an operating range of 30–200 Hz and sensitivity of 54 pm/g. Song et al. [16] have investigated a two-dimensional FBG acceleration sensor with the orthogonal flexible hinge structure. The resonant frequencies of the sensor in the X and Y directions are 1275 Hz and 1482 Hz and the sensitivities are 41.2 and 34.5 pm/g, respectively. Zhang et al. [17] have designed a broadband high-sensitivity FBG accelerometer consisting of a double diaphragm and H-hinge showing the maximum sensitivity of 40.3 pm/g in the range of 1–1000 Hz.

In spite of recent development of different types of hinge type acceleration sensors, it is still difficult to achieve high sensitivity and a broad frequency range at the same time. Therefore, it is necessary to come up with a new design to meet practical requirements. Herein, a symmetrical double hinge structure is designed to utilize double mass synchronous vibrations to improve the sensitivity. The finite element method is used to optimize the structure the sensor and the acceleration sensor is designed and fabricated according to the simulation results. The experimental results show that the acceleration sensor has a relatively flat response in the frequency range of 50 ~ 600 Hz and the sensitivity is 300 mV/g at 600 Hz.

Sensor design

Structural model

The double-hinge structure is illustrated in Fig. 1. The two inertial masses are distributed on both sides and the FBG is pasted on the upper surface of the mass block and suspended. In order to analyze the acceleration sensing characteristics of the structure, the mechanical model is constructed as shown in Fig. 2.

When the acceleration direction is along the z-axis, the inertial masses rotate at a small angle θ centered on the hinge. As shown in Fig. 2, the torque balance equation of the structure is:

$$maH - k_f \Delta L_f (h + r) - K_z \theta = 0 \tag{1}$$

where m is the inertial mass, K_z is the stiffness of the hinge, H is the distance between the center of the hinge and center of the inertial mass, h is the height of the inertial mass, and the displacement of the optical fiber is ΔL_f. The FBG is regarded as a spring with an elastic stiffness of k_f.

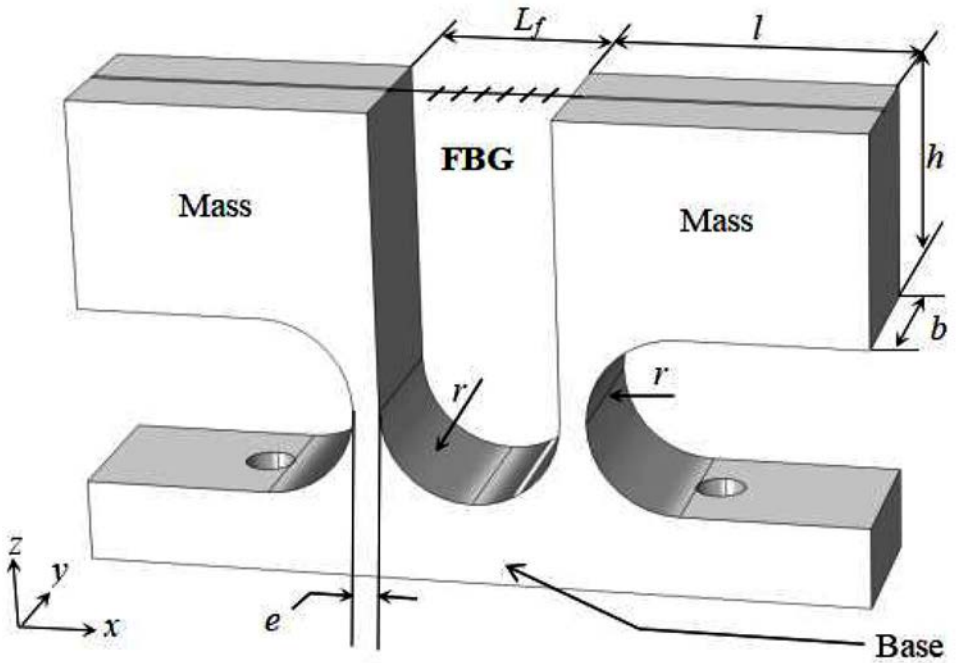

Fig. 1 Schematic structure of the sensor

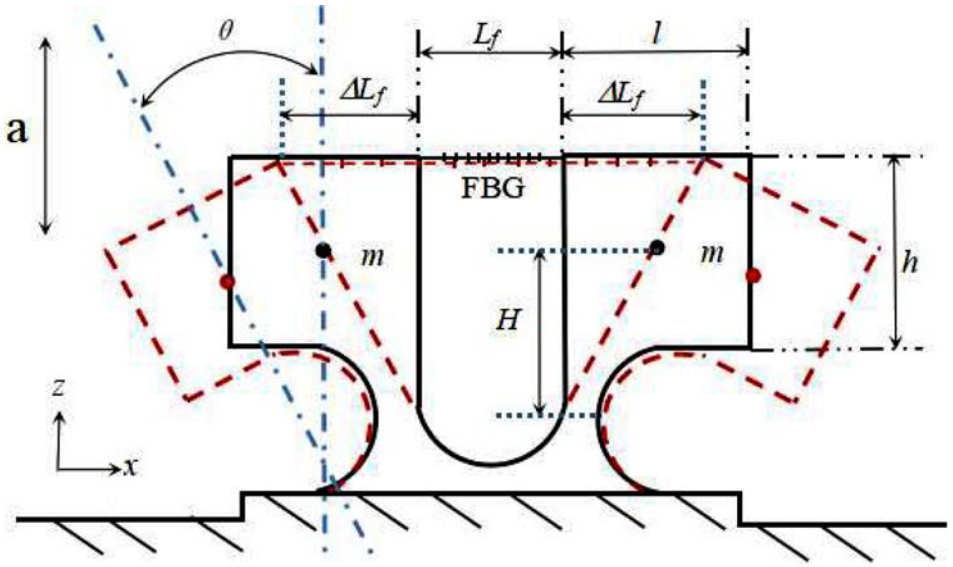

Fig. 2 Mechanical model of the structure

The stiffness of the elastic hinge can be expressed as [18]:

$$K_z = \frac{Ebr^2}{12} \Big/ \left[\frac{2s^2(6s^2+4s+1)}{(2s+1)(4s+1)^2} + \frac{12s^4(2s+1)}{(4s+1)^{5/2}} \arctan \sqrt{(4s+1)} \right] \tag{2}$$

where E and b are the Young's modulus and width of the inertial mass, r and e are the radius and thickness of the hinge, and $s = r / e$. The elastic stiffness of the optical fiber is:

$$k_f = \frac{E_f A_f}{L_f} \tag{3}$$

where, E_f is the elastic modulus of the optical fiber, A_f is the cross-sectional area, and L_f is the length of the suspended optical fiber. The Bragg wavelength shift $\Delta\lambda$ of the FBG is:

$$\frac{\Delta\lambda}{\lambda} = (1 - p_e)\,\varepsilon \tag{4}$$

where, p_e is the elastic optical coefficient of the optical fiber and ε is the axial strain.

Since the rotated angle θ is usually small, the FBG displacement caused by vibrations can be approximated by:

$$\Delta L_f = (r + h)\,\theta \tag{5}$$

Therefore, the axial strain ε of the FBG is:

$$\varepsilon = \frac{(r+h)\theta}{L_f} \tag{6}$$

The sensitivity of the sensor can be obtained by the following equation:

$$S = \frac{\Delta\lambda}{a} = 2(1 - p_e)$$
$$\frac{\lambda\varepsilon}{a} = \frac{2(1-p_e)\lambda m H(r+h)}{L_f[k(r+h)^2 + K]} \tag{7}$$

The natural frequency of the structure determines the operating frequency range of the sensor and the natural frequency f of the structure can be expressed as [19]:

$$f = \frac{1}{2\pi}\sqrt{\frac{k_f\left(\frac{h}{2}+r\right)^2 + K_z}{J}} \tag{8}$$

,where J is the moment of inertia of the hinge structure which can be expressed as [20]:

$$J = m\frac{h^2+l^2}{12} + m\left(\frac{h}{2}+r\right)^2 \tag{9}$$

According to the above theoretical analysis, the sensitivity S and natural frequency f depend on the structure. Considering the structural design and size constraints, the structural parameters are shown in Table 1. The sensitivity and natural frequency are calculated by Eqs. (7) and (8) to be 162.02 pm/g and 671.94 Hz, respectively.

Table 1 Parameters of the sensor

Symbols	Parameters	Values
E	Young's modulus of material	210 GPa
μ	Poisson's ratio of material	0.3
ρ	Density of material	7 800 kg/m^3
l	Length of mass	18.5 mm
b	Width of mass	10 mm
h	Height of mass	13 mm
λ	FBG center wavelength after packaging	1 552.27 nm
E_f	Young's modulus of the fiber	73 GPa
P_e	effective elastic-optical coefficient	0.22
L_f	the effective length of the fiber	11 mm
A_f	Cross-sectional area of an optical fiber	1.23×10^{-8}mm

Simulation

The finite element method is employed to analyze the sensing characteristics of the sensor with the structural parameters listed in Table 1. The lower surface of the structure has the fixed constraint boundary conditions. As z-axis acceleration is 5 m/s^2, the strain deformation and displacement distribution of the structure are shown in Fig. 3. The position of the hinge generates maximum strain and the resonant frequency is 670.211 Hz as shown in Fig. 3(a). The displacement exhibits a fan-shape distribution with the maximum observed from the upper surface of the inertial masses as shown in Fig. 3 (b) and (c). Therefore, the FBG is pasted here, the maximum displacement is about 2.5×10^{-4} mm. Meanwhile, the displacement direction of the two inertial masses is opposite, meaning that the strain sensitivity of the two-hinge structure is twice that of the single-hinge structure. Meanwhile in the presence of x-direction, the two inertial masses move along the same direction. The y-direction acceleration results in no displacement on the inner surface of the central U-shape. Therefore, this structure is insensitive to x- and y-direction vibrations.

In order to study the effects of the structural parameters on the frequency response range and sensitivity, the thickness e of the hinge, length l, width b, and height h of the inertial mass block are discussed. The curves of the natural frequency and hinge strain versus thickness e of the hinge in Fig. 4(a) show that the natural frequency of the sensor increases almost linearly with the hinge thickness e, but the strain decreases exponentially. Therefore, the sensor has higher sensitivity and lower frequency response for a smaller e. In order to increase frequency response and retain the high sensitivity, the fatigue resistance of the hinge, $e=1$ mm, is chosen as the optimal value. The influence of length l of the inertial mass block on the sensing performance is analyzed as shown in Fig. 4(b). With increasing l, the natural frequency decreases approximately linearly, whereas the strain increases rapidly at first and then slowly thereafter. To obtain higher dynamic response frequency and better sensitivity, $l=18.5$ mm is taken as the optimal value. In the same way, the width b and height h of the inertial mass block are analyzed as shown in Fig. 4(c) and (d), respectively, and $b=10$ mm and $h=13$ mm are selected.

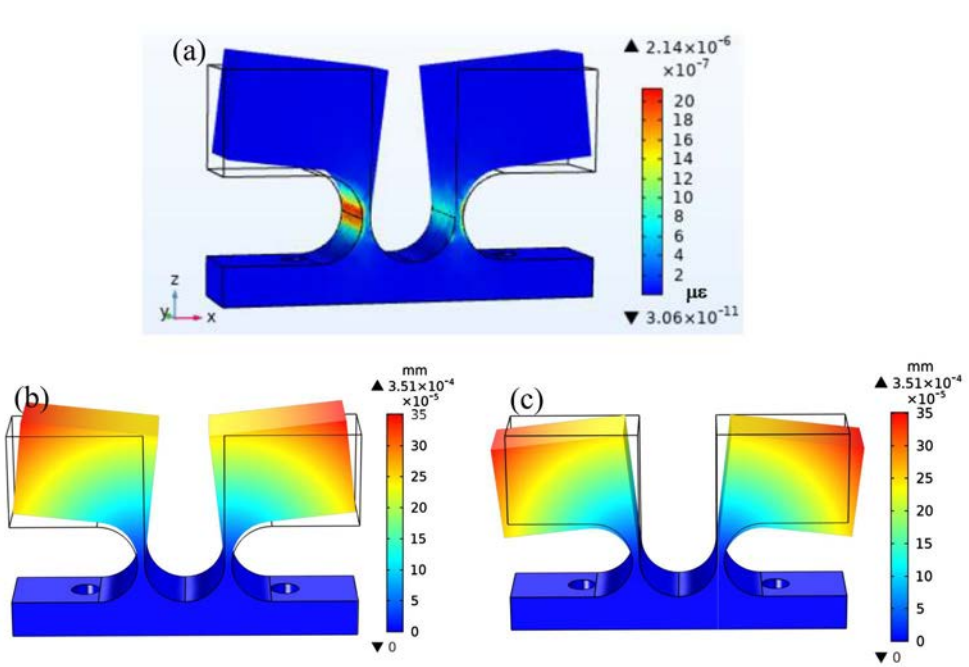

Fig. 3 Finite element analysis (**a**) Strain distribution of the natural frequency at 5 m/s^2, (**b**) and (**c**) Displacement distribution of the structure for z-direction vibration

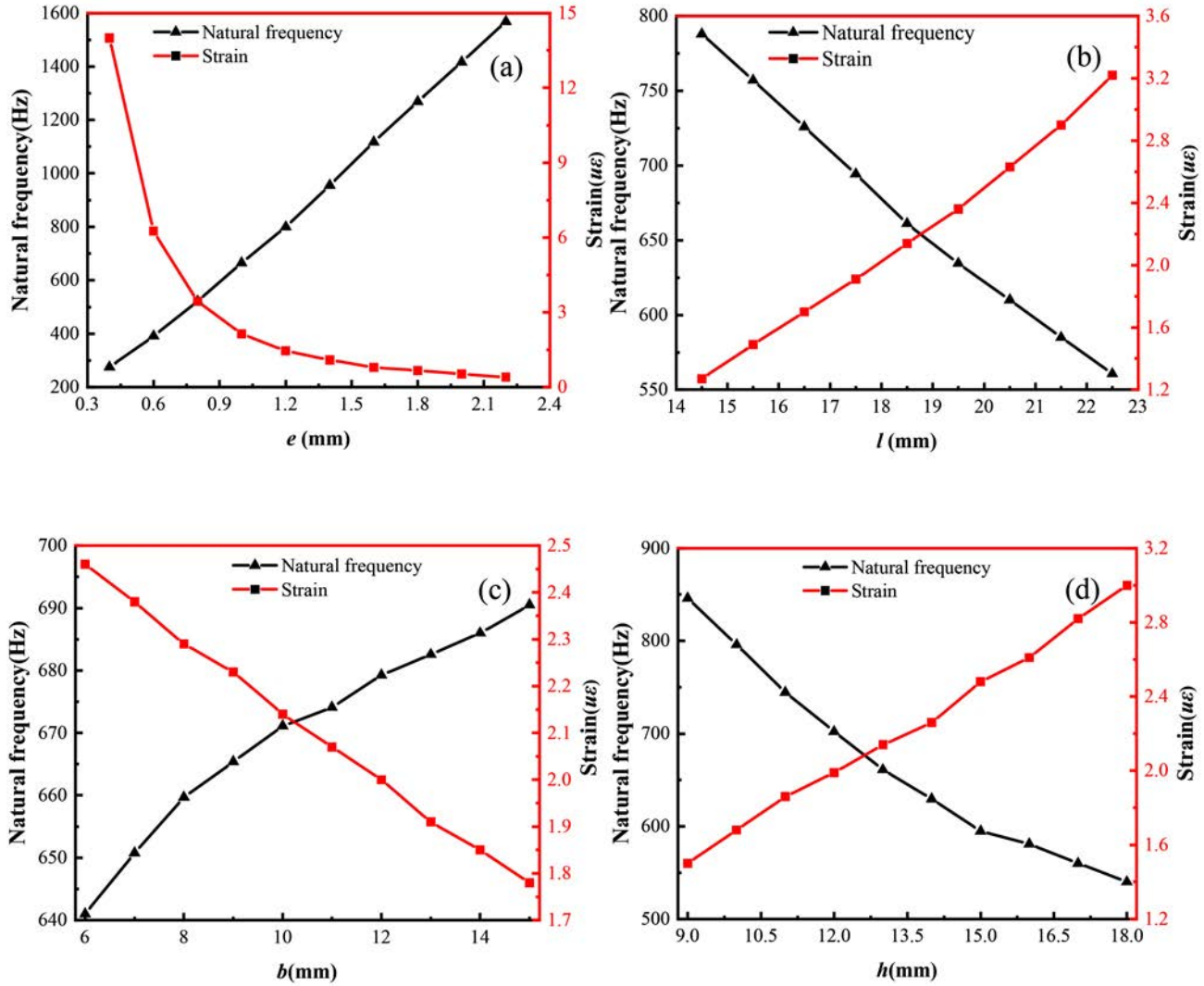

Fig. 4 Natural frequency and hinge strain versus different structural parameters: (**a**) Thickness *e* of the hinge, (**b**) Length *l*, (**c**) Width *b*, and (**d**) Height *h*

Experimental analysis

The double-hinge structure is constructed using 304 stainless steel and fixed on a high-precision vibration table as shown in Fig. 5. The vibration table can provide vertical acceleration of 0–5 kHz and 0–10 g. The conventional FBG with axial prestress is pasted and suspended between the two inertial masses [21]. The self-developed low-cost edge filter demodulation system based on the long-period fiber grating (LPFG) including the ASE broadband light source, LPFG, 3dB coupler, and photoelectric detector is used to detect the wavelength shifts of FBG [22]. The data are analyzed by an oscilloscope.

The frequency response of the acceleration sensor is determined. As the standard sine wave vibration signal is added to the vibration table with the 1 g z-axis acceleration, the resulting waveforms of 200 Hz, 400 Hz, 600 Hz are shown in Fig. 6(a). The vibration signals are detected but the amplitudes of the signals are different. Therefore, the amplitude-frequency response is monitored using the peak-to-peak value of the vibration signal in the range of 50 ~ 1000 Hz as shown in Fig. 6(b). The maximum amplitude appears at 670 Hz corresponding to the resonance frequency of the structure. In the lower vibration frequency range of 50 ~ 600 Hz, the sensor exhibits a relatively flat response implying that the sensor is functional in this range. The experimental results are in good agreement with the theoretical assessment.

The acceleration-amplitude relationship is determined by monitoring the peak-to-peak signals as shown in Fig. 7 which reveals that the peak-to-peak values increase linearly. Hence, a linear function is implemented to fit the relationship

Fig. 5 Experimental setup

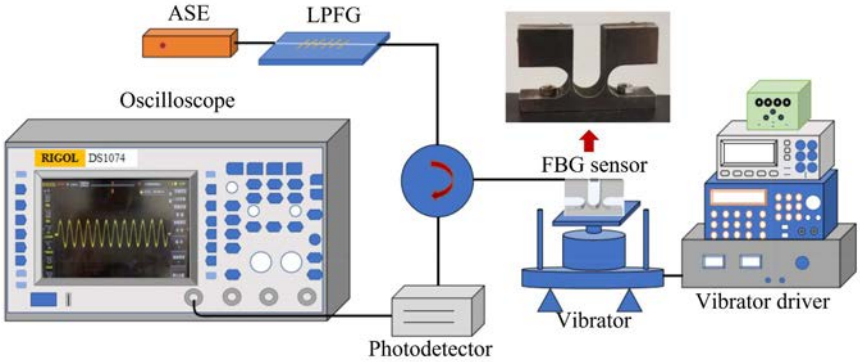

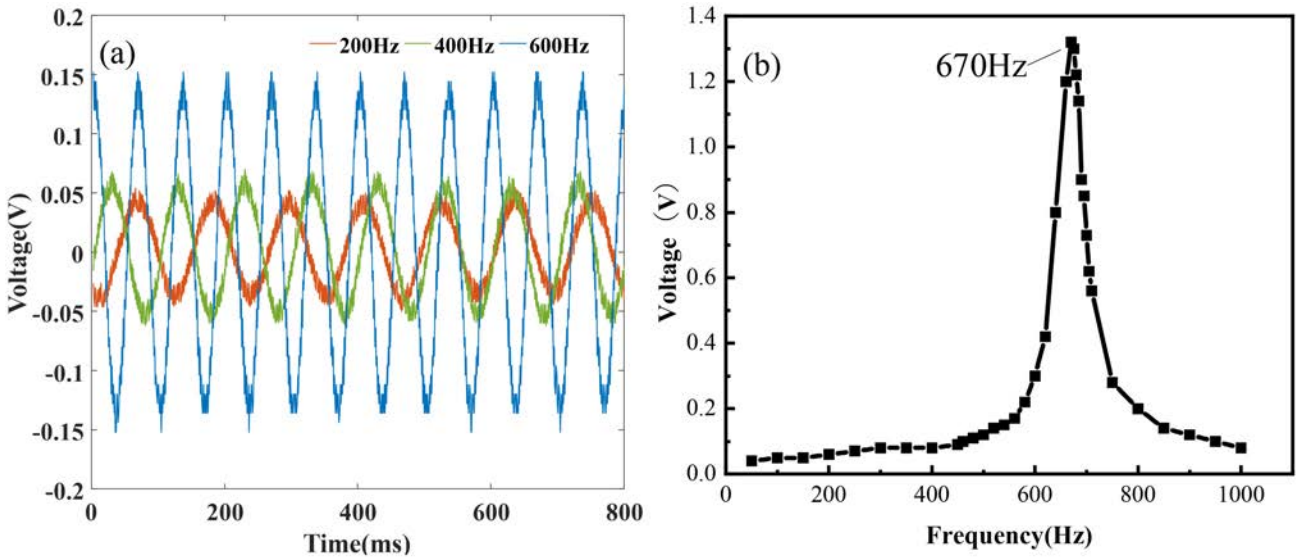

Fig. 6 Amplitude-frequency response of the sensor: (**a**) Response curves of FBG at 200 Hz, 400 Hz, and 600 Hz and (**b**) Amplitude frequency curve

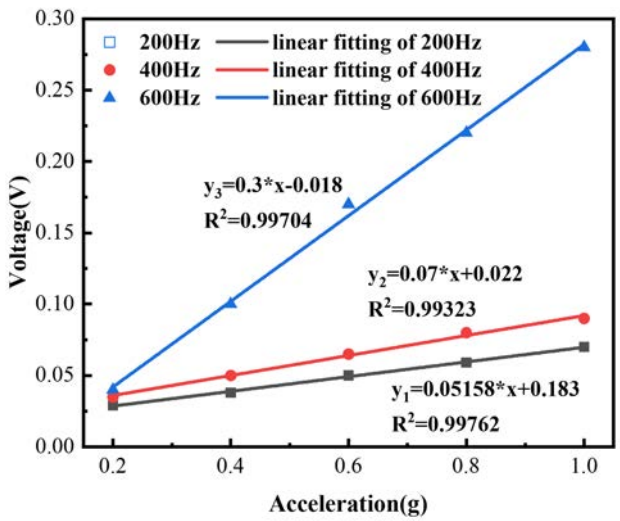

Fig. 7 Acceleration sensitivity of the sensor

and the slope is 300 mV/g at 600 Hz with $R^2 = 0.99704$. The sensitivity of the sensor is thus 300 mV/g. Similarly, the characteristics of the sensor are analyzed at 200 Hz and 400 Hz and sensitivities of 51.58 mV/g and 70 mV/g are achieved, respectively.

Resolution is an important factor in the detection of weak vibrations. Figure 8 shows the amplitude spectra in Fig. 7(a) in the frequency domain for acceleration and vibration frequencies of 1 g and 600 Hz respectively. The signal-to-noise ratio (SNR) is about 60 dB and the resolution is approximately 1 mg/Hz$^{1/2}$. It is noted that the sensor characteristics derived by the demodulation method of the FBG suggest that the noise can be reduced and suppressed by changing the demodulation method [23]. Hence, the SNR and sensor resolution can be improved further in the future.

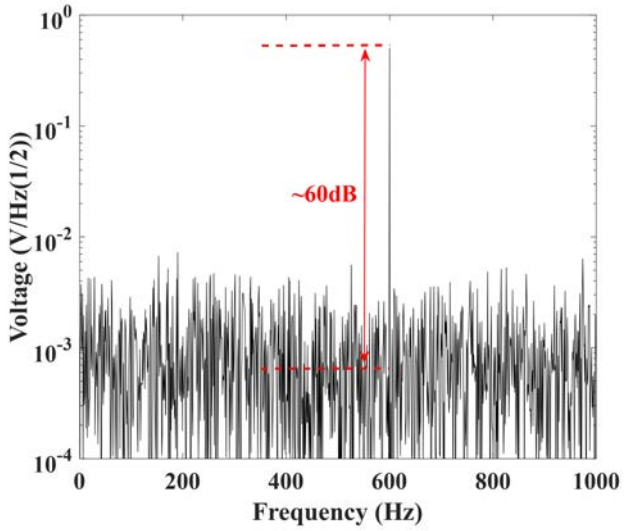

Fig. 8 Amplitude spectrum acquired at 600 Hz vibration frequency and 1 g acceleration

Conclusion

A fiber Bragg grating (FBG) acceleration sensor with the double-hinge structure boasting a wide dynamic range is designed and analyzed. Analysis based on the theoretical model verifies that the symmetrical structure improves the sensitivity and frequency response range of the sensor. The finite element method is utilized to optimize the structure and the optimal senor is prepared experimentally based on the best structural parameters. The assembled sensor is investigated experimentally and the sensitivity and resolution are found to be 300 mV/g and 1 mg/Hz$^{1/2}$ at 600 Hz and the dynamic range is 50∼600 Hz. Because of the flexible design, the sensing performance can be further improved by using better demodulation methods.

Acknowledgements This work was jointly supported by the instructional Technology Plan of Daqing City [zd-2023-19], Daqing Normal University Talent Project[22RC006], Hainan Province Science and Technology Special Fund [ZDYF2022GXJS003], Postdoctoral Scientific Research Development Fund of Heilongjiang Province [LBHQ20081], Local Universities Reformation and Development Personnel Training Supporting Project from Central Authorities [140119001], City University of Hong Kong Donation Research Grant [DON-RMG 9229021], City University of Hong Kong Strategic Research Grant [SRG 7005505], as well as City University of Hong Kong Donation Grant [9220061].

Declarations

Conflict of interest The authors declare no conflicts of interest.

References

1. S.R. Xie, Q.L. Zou, L.W. Wang et al., Positioning error prediction theory for dual Mach-Zehnder interferometric vibration sensor. J. Lightwave Technol. **29**(3), 362–368 (2011)
2. Y. Yang, E. Wang, K. Chen et al., Fiber-optic fabry-perot sensor for simultaneous measurement of tilt angle and vibration acceleration. IEEE Sens. J. **19**(6), 2162–2169 (2019)
3. C. Zhao, D. Liu, K. Xu et al., Recent advances in fiber optic sensors for respiratory monitoring. Opt. Fiber Technol. **72**, 103000 (2022)
4. X.F. Zhao, Z.A. Jia, W. Fan et al., A Fiber Bragg grating acceleration sensor with temperature compensation. Optik. **241**, 166993 (2021)
5. S.X. Jiao, Y. Zhao, J.J. Gu, Simultaneous measurement of humidity and temperature using a polyvinyl alcohol tapered fiber Bragg Grating. Instrum. Sci. Technol. **46**(5), 463–474 (2018)
6. M. Yang, Q.D. Liu, H.S. Naqawe et al., Movement detection in soft robotic gripper using sinusoidally embedded fiber optic sensor. Sensors. **20**(5), 1312 (2020)
7. Z.A. Jia, X.F. Zhao, W. Fan et al., A two-dimensional cantilever beam vibration sensor based on fiber Bragg Grating, Opti. Fiber Technol. **61**(5), 102447 (2021)
8. J. Zhu, J. Wang, P. Gan et al., Design and analysis of a Novel Dual FBG Accelerometer based on Lantern shape metallic shells. IEEE Sens. J. **17**(16), 5130–5135 (2017)
9. L. Wei, D.Z. Jiang, L.L. Yu et al., A Novel Miniaturized Fiber Bragg Grating Vibration Sensor. IEEE Sens. J. **19**(24), 11932–11940 (2019)
10. Y.S. Zhang, X.G. Qiao, Q.P. Liu et al., Study on a Fiber Bragg Grating Accelerometer based on compliant cylinder, Opti. Fiber Technol. 26(part B), 229–233(2015)
11. T.L. Li, J.X. Guo, Y.G. Tan et al., Recent advances and tendency in fiber Bragg grating-based vibration sensor: a review. IEEE Sens. J. **20**(20), 12074–12087 (2020)
12. Y.S. Zhang, W.G. Zhang, Y.X. Zhang et al., A two-dimensional medium-high frequency Fiber Bragg Gratings Accelerometer. IEEE Sens. J. **17**(3), 614–618 (2017)
13. L. Qiu, L. Liang, D.X. Li et al., Theoretical and experimental study on FBG accelerometer based on multi-flexible hinge mechanism. Opt. Fiber Technol. **38**, 142–146 (2017)
14. L. Wei, L.L. Yu, J.J. Wang et al., An FBG-Sensing two-dimensional vibration Sensor based on Multi-axis Flexure Hinge. IEEE Sens. J. **19**(10), 3698–3710 (2019)
15. B. Yan, L. Liang, A Novel Fiber Bragg Grating Accelerometer based on parallel double flexible hinges. IEEE Sens. J. **20**(9), 4713–4718 (2020)
16. H. Song, Q.D. Wang, M.Y. Liu et al., A Novel Fiber Bragg Grating Vibration Sensor based on Orthogonal Flexure Hinge structure. IEEE Sens. J. **20**(10), 5277–5285 (2020)
17. F.X. Zhang, S.D. Jiang, C. Wang et al., Broadband and High Sensitivity FBG Accelerometer based on double diaphragms and h-Shaped hinges. IEEE Sens. J. **21**(1), 353–359 (2021)
18. J.L. Gong, Y.F. Zhang, K. Mostafa et al., Accurate stiffness modeling method for Flexure hinges with a complex contour curve. Micro Nanosystems. **13**(1), 24–31 (2021)
19. B.X. Hu, G.D. Song, F. Zhu et al., Fiber Optic Microseismic Monitoring System used in Underground Coal Mines. J. Phys. Conf. Ser. **1065**(25), 252012 (2018)
20. Z.W. Zhu, X.Q. Zhou, R.Q. Wang et al., A simple compliance modeling method for flexure hinges. Technol. Sci. **58**(1), 56–63 (2015)
21. Y. Wang, Z.L. Zhang, Y.Y. Sun et al., The influence of different surface paste on FBG strain transfer. Piezoelectrics Acoustooptics. **38**(1), 106–110 (2016)

22. Q. Liu, B.W. Li, Y.D. Sun et al., Study on FBG demodulation method based on long-period Fiber grating. J. Appl. Opt. **43**(1), 160–166 (2022)
23. F.X. Zhang, C. Wang, S.D. Jiang et al., Dynamic fiber Bragg grating sensor array with increased wavelength-division multiplexing density and low crosstalk. Opt. Eng. **56**(3), 037101 (2017)